Laser Interferometric Technique for Measuring Polymer Cure Kinetics

O. DUDI, W. T. GRUBBS

Stetson University, Department of Chemistry, Unit 8271, DeLand, Florida 32720

Received 14 September 1998; accepted 28 February 1999

ABSTRACT: An optical interference apparatus for the analysis of polymer curing kinetics is described. The device employs a helium-neon laser and a home-built Michelson interferometer to measure refractive index variations and film thickness variations during film polymerization. The refractive index variation provides a phenomenological measure of the extent of cure. The technique is demonstrated by collecting interferometric curing profiles for a UV photocurable acrylate resin formulation. Systematic comparisons of curing profiles are made as a function of UV illumination intensity and photoinitiator concentration. Several aspects of the curing process are characterized by these interferometric measurements, such as film shrinkage, gel point formation, and the kinetics of photopolymerization inhibition. © 1999 John Wiley & Sons, Inc. J Appl Polym Sci 74: 2133–2142, 1999

Key words: photopolymerization; cure kinetics; refractive index; UV curing; interferometry

INTRODUCTION

The UV photocurable coatings industry has flourished for nearly 30 years. The popularity of photocurables can be attributed to several aspects of these coatings. First, the availability of a wide range of functionalized monomers and oligomers allows one to readily tailor the properties of photocurables to meet specific applications. Second, the formulations are environmentally friendly, consisting of 100% reactive, nonvolatile components. Third, photocuring is rapid and energy efficient in comparison to conventional thermal curing. (Photocurables can be formulated to cure within a second upon illumination with standard UV sources.) Fourth, the photopolymerization process in itself can impart properties to a coating that are difficult to achieve by thermal curing. These combined characteristics make photocurables a versatile coatings class that can be applied to wood, metal, and plastic substrates. A number of excellent reviews have been published on UV photocuring.[1–4]

The measurement of cure rate in photocurable coatings can be difficult to achieve by conventional methods. The rapid progression of the photocured sample from a liquid state through a gelatinous stage to an insoluble solid state can be difficult to follow with any one technique. Consider IR and UV spectroscopy, which are often used to follow the extent of reaction during polymerization.[3,5,6] Variations in the refractive index can occur during cure and can alter the reflection (transmission) of light at (through) the polymer film surface, giving rise to IR and UV absorption transients that are not directly related to the extent of the reaction. Consequently, the interpretation of the transient data is nontrivial. This problem is particularly troublesome when attempting to apply transient spectroscopy to the study of long time scale densification in polymers. A number of other standard techniques, such as ellipsometry,[7,8] dilatometry,[9] linear expansion

Correspondence to: W. T. Grubbs.
Contract grant sponsor: Petroleum Research Fund.

Journal of Applied Polymer Science, Vol. 74, 2133–2142 (1999)
 CCC 0021-8995/99/092133-10

measurements,[10] and shear modulus measurements[11] possess limitations that hinder their use in photocuring studies. Calorimetric techniques,[5,12,13] such as DSC or thin-foil measurements of heat evolution, have been somewhat successful in following photopolymerization. These thermal methods display a high sensitivity to the initial, highly exothermic portion of a polymerization reaction. However, they exhibit only a limited sensitivity to slow physical relaxation processes that occur beyond the gel point of a polymer, such as densification. The ability to probe physical relaxation processes is of considerable technological importance; densification is a manifestation of structural relaxation and free volume shrinkage, which reduce internal stress in a polymer network and thereby minimize cracking and peeling of a film from its substrate.[10,14]

This article describes a newly constructed optical interference apparatus, which is based on a low power helium-neon laser and a Michelson interferometer, that can be used to follow curing processes in a polymer film. Specifically, the apparatus allows one to measure the time derivatives of refractive index ($\Delta n/\Delta t$) and film thickness ($\Delta l/\Delta t$) during the curing process. The variation in $\Delta n/\Delta t$ as the reaction proceeds provides a phenomenological curing profile. The variation in $\Delta l/\Delta t$ as a function of cure time provides a measure of the kinetics of film shrinkage. Unlike many previously available methods, interferometric measurements are expected to be sensitive to curing processes over the full course of the reaction. Because the Lorentz–Lorenz formula[15] predicts a strong correlation between the refractive index and density, interferometric post gel point densification studies should be possible.

The study described here is not the first refractive index investigation of polymer cure. An Abbe refractometer was used in earlier investigations to measure the *absolute* refractive index at different points during the curing reaction.[16,17] Although the interferometric method described here cannot be used to measure the *absolute* refractive index in a material, it is highly sensitive to refractive index *variations.* The interferometric measurements of $\Delta n/\Delta t$ described here are 2 orders of magnitude more sensitive than Abbe refractometer measurements of $\Delta n/\Delta t$. More recently, a holographic grating technique[18] was developed that allows one to measure the refractive index change that accompanies laser-induced polymerization. In comparison to interferometry, this technique is intrinsically less sensitive to refractive index variations; this holographic method involves the scattering of one laser beam by a refractive index grating that is generated by the interference of two other laser beams (a third-order optical process). Also, the photoinitiation wavelength in a holographic experiment is restricted to the wavelength of the laser that is used to write the grating.

The objective of the present work is to demonstrate the effectiveness of this interferometric technique for monitoring photopolymerization kinetics. Curing profiles are collected at different UV illumination intensities and photoinitiator concentrations for a simple photocurable acrylate resin formulation. Analysis of the curing profiles permits the characterization of several aspects of the curing process, such as the extent of cure, gel point formation, film shrinkage, and the inhibition of photopolymerization.

EXPERIMENTAL

Materials

The photocurable formulation investigated here was a mixture of an acrylate resin, dipentaerythritol pentaacrylate (DPEPA, from Sartomer Company, Inc.), and a liquid photoinitiator, 2-hydroxy-2-methyl-1-phenyl-1-propanone (Darocur 1173, from Ciba–Geigy). Both components were used as received without further purification. The DPEPA resin contains 270 ppm of methoxyhydroquinone (MEHQ) to inhibit self-polymerization. The three samples prepared for study contained 2.0, 4.0, and 8.0% by volume photoinitiator. All photocuring studies were conducted at ambient temperature ($\sim$ 22°C).

UV Curing Source

A 150-W xenon arc lamp (Oriel Corp.) and a high intensity single grating monochromator (Bausch and Lomb model 33-86-79, 1350 grooves/mm of grating, blazed at 300 nm) were used in tandem to produce photoinitiation light at 360 nm. This radiation was loosely focused with a 30-cm focal length lens (Fig. 1) to produce a spot size at the sample that was roughly 20 times larger than the $\sim$ 1-mm laser beam spot size; consequently, one can assume that the sample was uniformly irradiated over the width of the laser beam. This arrangement yielded an UV power density at the sample of approximately 0.05 mW/cm^2. The photocurable samples were only weakly absorbent at the chosen photoinitiation wavelength of 360 nm.

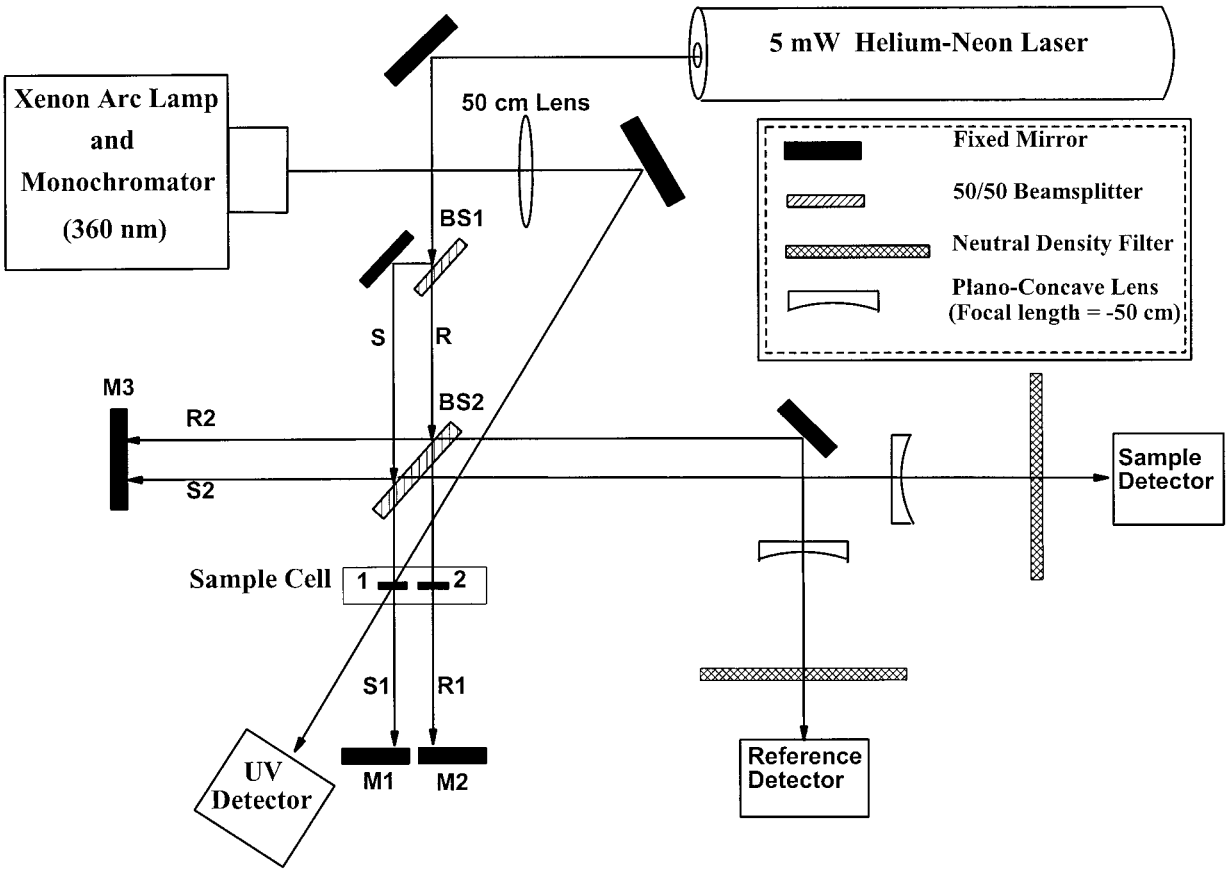

Figure 1 Schematic diagram of the interferometric apparatus. The Xe arc lamp/monochromator and its power supply are mounted on a separate table for vibration isolation.

(The measured absorbance was less than 0.1 for the uncured 200-μm samples studied here.) This wavelength coincides with the low-frequency tail of the photoinitiator absorption peak. As such, the reduction in UV excitation intensity is negligible through the sample and photocuring is uniform through the 200-μm thickness of the films.

Interferometric Instrument

The experimental apparatus illustrated in Figure 1 was assembled on a vibration free optical table. When a polymerizing film was placed in one arm of the Michelson interferometer, the variations in refractive index and film thickness caused a corresponding change in the phase of the coherent optical beam that passes through the film; the output of the interferometer subsequently fluctuated between constructive and destructive interference. The oscillations in the interferometer output intensity were monitored with a photodiode. The times that transpired between successive maxima (or minima) in this "interferogram" were used to calculate the time derivatives of the refractive index ($\Delta n/\Delta t$) and film thickness ($\Delta l/\Delta t$) throughout the curing process.

Referring to Figure 1, coherent light from a helium-neon laser (5 mW, λ = 632.8 nm) is split with a 50/50 beamsplitter (BS1) into sample (S) and reference (R) beams. These beams are split again with a second 50/50 beamsplitter (BS2), creating two pairs of beams for the Michelson interferometer, that are hereafter called S1, S2, R1, and R2. S1 and R1 are the "sample" and "reference" beams, respectively, that pass through the sample cell. These beams are subsequently reflected back to beamsplitter BS2 by adjacent mirrors M1 and M2. (These mirrors are positioned about 10 cm from beamsplitter BS2.) Beams S2 and R2 travel approximately 10 cm to a separate mirror, M3, where they are reflected back to beamsplitter BS2. The intensity of light that results from the interference of beams S1

and S2 is monitored with a battery powered photodiode/amplifier chip (part OPT101, Burr-Brown Corp., Tucson, AZ, sample detector in Fig. 1). The interference of beams R1 and R2 is monitored with a separate detector (reference detector).

The intensity of light at the sample detector, or the reference detector, is dependent on the difference between the pathlengths traveled by beams S1 and S2, or beams R1 and R2, respectively. For example, if the pathlength difference between S1 and S2 is an exact multiple of the wavelength of the laser light, the recombined beams will interfere constructively and a corresponding maximum intensity will be observed at the sample detector.

All mirror positions were fixed during our measurements. Consequently, any variation in interference was a result of the polymerization reaction in the sample cell. It is useful to define a vacuum pathlength of light through the sample (p), which is given by the product of the film thickness (l) and the refractive index of the film (n),

$$p = ln \tag{1}$$

Polymerization will cause changes in l and n, and the corresponding variation in vacuum pathlength is

$$dp = n\ dl + l\ dn \tag{2}$$

In the interest of describing how n, l, and p vary over time, eq. (2) is divided by dt to obtain

$$\frac{dp}{dt} = n\frac{dl}{dt} + l\frac{dn}{dt} \tag{3}$$

Replacing the differentials (d) with deltas (Δ) and additional rearrangement gives an expression that describes "macroscopic" variations in the refractive index with time:

$$\frac{\Delta n}{\Delta t} = \frac{1}{l}\frac{\Delta p}{\Delta t} - \frac{n}{l}\frac{\Delta l}{\Delta t} \tag{4}$$

The interferometric method presented here is based on eq. (4); the interferogram collected at the sample detector was used to determine values of $\Delta p/\Delta t$, the interferogram collected at the reference detector was used to determine values of $\Delta l/\Delta t$, and these quantities were then used to calculate $\Delta n/\Delta t$ at different points throughout the reaction.

The calculation of $\Delta n/\Delta t$ in this fashion requires the use of an interferometric cell that holds two adjacent samples, only one of which was photocured. The $\Delta p/\Delta t$ and $\Delta l/\Delta t$ were determined separately by simultaneously collecting interferograms for the cured and uncured samples, respectively. As illustrated in Figure 1, the cell is mounted in the interferometer such that beam S1 passes through sample 1 and beam R1 passes through sample 2. (Samples 1 and 2 are approximately 1.25 cm apart.) The cell used here consisted of two 3×3 cm^2 microscope slide windows and a 200-μm Teflon spacer. A stirring bar was used to apply two spots of the viscous photocurable sample to one window. The Teflon spacer was fitted into place and then the two windows were loosely sandwiched together inside a threaded metal retainer. The relatively soft Teflon spacer and the fact that the cell was not tightly sandwiched allowed the cell to contract over a small distance with film shrinkage. When sample 1 was photocured, the subsequent variations in l and n caused the intensity of light at the sample detector to vary according to $\Delta p/\Delta t$. Sample 2, which was not photocured, retained a constant refractive index. However, the reference interferogram still exhibited oscillations because the polymerization of sample 1 pulls the windows together, causing the pathlength of sample 2 to shrink according to $\Delta l/\Delta t$.

The sample and reference detector voltages were collected as a function of time through two channels of an analog to digital computer acquisition interface. The amount of UV light transmitted through the sample was also monitored with a third photodiode/amplifier chip in order to establish the starting time of the curing process. (The voltage from this detector was monitored by a third channel of the computer interface.) A 10-Hz data acquisition rate was utilized for these measurements.

Temperature stability can be difficult to maintain during photocuring studies because of the rapid, highly exothermic nature of the reaction. The small sample volumes employed here (1–2 drops) and the large surface area of the samples (in contact with the glass windows) helped to maintain an isothermal environment. A small thermocouple was used to test the temperature stability inside the sample cell upon photocuring, revealing a maximum temperature increase of only 0.5°C.

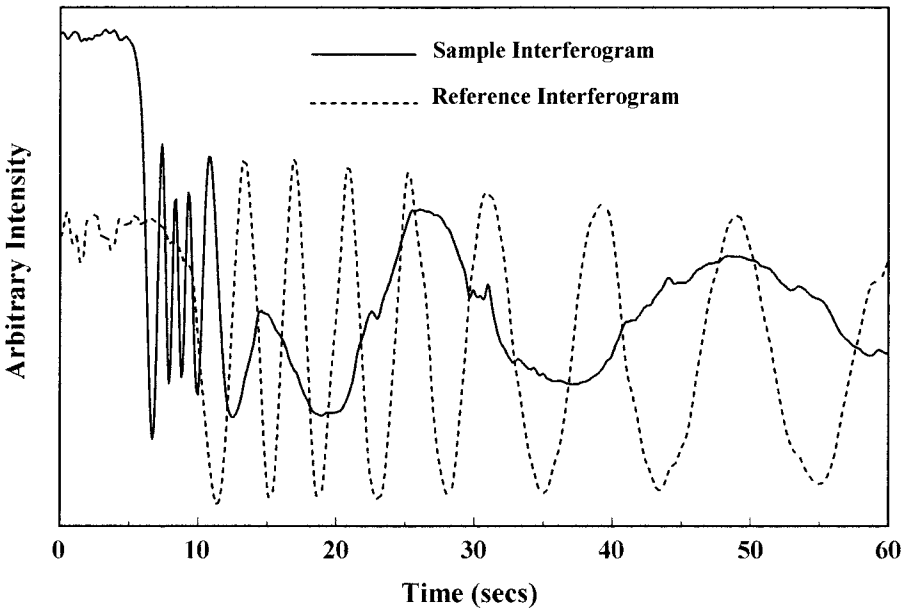

Figure 2 Sample and reference interferograms of a DPEPA sample containing 4.0% by volume Darocur 1173 and a UV irradiation power density of 0.054 mW/cm^2.

RESULTS AND DISCUSSION

Interferogram Analysis

Figure 2 shows typical sample and reference interferograms collected for a photocurable mixture containing 4.0% Daracur 1173 by volume and a UV irradiation power density of 0.054 mW/cm^2. Several seconds transpired between UV illumination and the onset of oscillations in the interferograms. This time lag was due to inhibition of the polymerization reaction by dissolved oxygen and possibly the MEHQ resin inhibitor. (Inhibition by molecular oxygen and MEHQ is a well-known phenomenon and was addressed in previous investigations.[19–22] Inhibition kinetics in these samples will be discussed in a later section.

As can be seen in Figure 2, the sample interferogram begins to oscillate before the reference interferogram. This indicates that film shrinkage is delayed relative to the beginning of the photocuring reaction. This delay was expected: the initial addition of monomers produced a refractive index increase in the sample that caused the sample interferogram signal to oscillate; yet, oscillations in the reference interferogram signal will not occur until the polymer reaction enters the crosslinking phase, which gives rise to film shrinkage.

To obtain a curing profile the *sample* interferogram data were first inspected to determine the time at which each maximum and minimum occurs. (This task was facilitated by loading the interferogram data into a computer spreadsheet.) These times were used to calculate $\Delta p/\Delta t$ throughout the photocuring reaction.

$$\frac{\Delta p}{\Delta t} = \frac{\lambda}{t_2 - t_1} \tag{5}$$

In this expression, $\lambda = 0.6328$ μm (the wavelength of the HeNe laser light) and $t_2 - t_1$ is the amount of time between successive maxima (or minima) in the sample interferogram. Each $\Delta p/\Delta t$ value was tabulated along with its "average" time, $(t_2 + t_1)/2$. The *reference* interferogram data were inspected in a similar fashion to evaluate

$$\frac{\Delta l}{\Delta t} = \frac{1}{n_r}\frac{\lambda}{(t_2 - t_1)} \tag{6}$$

where n_r is the refractive index of the uncured sample (sample 2) and $t_2 - t_1$ is the amount of time between successive maxima (or minima) in the reference interferogram. Each $\Delta l/\Delta t$ value was tabulated along with its average time, $(t_2 + t_1)/2$.

The series of $\Delta p/\Delta t$ and $\Delta l/\Delta t$ values were used to calculate $\Delta n/\Delta t$ values. According to eq. (4), the calculation of $\Delta n/\Delta t$ at an instant in time during the photocuring reaction not only requires $\Delta p/\Delta t$

and $\Delta l/\Delta t$ values, but also requires the absolute values of n and l. Yet, the values of n and l varied as the reaction proceeded. Abbe refractometer measurements of the absolute refractive index before and after cure revealed that n only varied by $\sim 2\%$ over the full course of the curing process. Similarly, the oscillations observed in the reference interferograms indicated that the film thickness only varied by $\sim 1\%$ in these systems. Consequently, it is fair to assume that n and l remain constant when using the right-hand side of eq. (4) to calculate $\Delta n/\Delta t$. The error associated with this assumption is small in comparison to other sources of error in this experiment and produced only a 2% uncertainty in the calculated $\Delta n/\Delta t$ values. The experimentally measured $t_2 - t_1$ values were the dominant source of error when determining $\Delta n/\Delta t$ values. (The uncertainty in $t_2 - t_1$ can be as high as 8% during the initial, rapid portion of the photopolymerization reaction, but it then decreases to less than 1% after the polymer passes through the gel point.) Because the absolute refractive index only changes by $\sim 2\%$, n_r in eq. (6) can be set equal to n in eq. (4). Consequently, the refractive index terms cancel when eq. (6) is substituted into eq. (4), which means the absolute refractive index of the medium is no longer needed to calculate $\Delta n/\Delta t$.

Although the refractive index term can be eliminated from eq. (4) by the arguments given above, the film thickness l is still required to calculate $\Delta n/\Delta t$. Polymer films were recovered at the conclusion of each experimental run by disassembling the sandwich cell and using a razor blade to "pop" the cured film loose from the microscope slide windows. The absolute film thickness was then measured to within $\pm 2\%$ with a precision micrometer. The value of l that is used in all calculations is twice the absolute film thickness. (The laser beams pass through the sample cell twice in a Michelson interferometer.) Again, it is important to note that the $\pm 2\%$ uncertainty in absolute film thickness $\Delta n/\Delta t$ makes a relatively small contribution to the overall uncertainty in the $\Delta n/\Delta t$ values.

Table I shows a sequence of $(1/l)\Delta p/\Delta t$ and $(n/l)\Delta l/\Delta t$ values that were determined from the interferograms in Figure 2, along with the subsequent $\Delta n/\Delta t$ values. The $\Delta n/\Delta t$ values were evaluated at the same instants in time as the available $(1/l)\Delta p/\Delta t$ values; the $(n/l)\Delta l/\Delta t$ values in Table I were obtained by linearly interpolating between available values. The series of $(n/l)\Delta l/\Delta t$ values were negative because the sample shrunk during cure. Alternatively, the $(1/l)\Delta p/\Delta t$ values were positive at the beginning of the reaction and became negative toward the end of the curing period. The sign of $\Delta p/\Delta t$ at any instant was determined by the relative signs of $\Delta n/\Delta t$ and $\Delta l/\Delta t$. Near the beginning of the curing reaction the refractive index rapidly increased whereas the film thickness remained constant, yielding positive values of $\Delta p/\Delta t$. As photocuring proceeded the refractive index increased less rapidly and the film began to shrink. At some intermediate time, the value of $\Delta p/\Delta t$ passes through zero as the negative value of the shrinkage term overtakes the positive value of $\Delta n/\Delta t$. This intermediate time can be identified in the sample interferogram as the point where the oscillations nearly stop and then begin again more slowly. It is important to correctly identify this "crossover" point in each sample interferogram so that the proper sign can be assigned to each calculated $(1/l)\Delta p/\Delta t$ value.

Table I Values Determined from Sample and Reference Interferograms in Figure 2

Time (s)	$\frac{1}{l}\frac{\Delta p}{\Delta t}$ (10^3/s)	$\frac{n}{l}\frac{\Delta l}{\Delta t}$ (10^3/s)	$\frac{\Delta n}{\Delta t}$ (10^3/s)
13.50	0	0	0
14.26	0.52	0	0.52
15.62	1.28	0	1.28
16.18	1.63	0	1.63
16.68	1.73	0	1.73
17.15	1.60	0	1.60
17.71	1.36	0	1.36
18.39	1.04	−0.06	1.11
19.58	0.60	−0.19	0.75
20.01	0.45	−0.23	0.68
31.32	−0.11	−0.35	0.24
36.30	−0.09	−0.28	0.19
45.96	−0.07	−0.19	0.12
59.36	−0.05	−0.13	0.08

An $\sim 8\%$ uncertainty exists for these $\Delta n/\Delta t$ values. The value of l is 404 ± 8 μm for this sample (twice the cured film thickness measured with a micrometer).

Film Shrinkage

Significant film shrinkage is expected to occur when the highly functional DPEPA is photocured (R. Obie, private communication, 1999). Intense photocuring of this resin can also produce film cracking. (In practice, this resin is normally blended with lower functionality oligomers to reduce stress formation.)

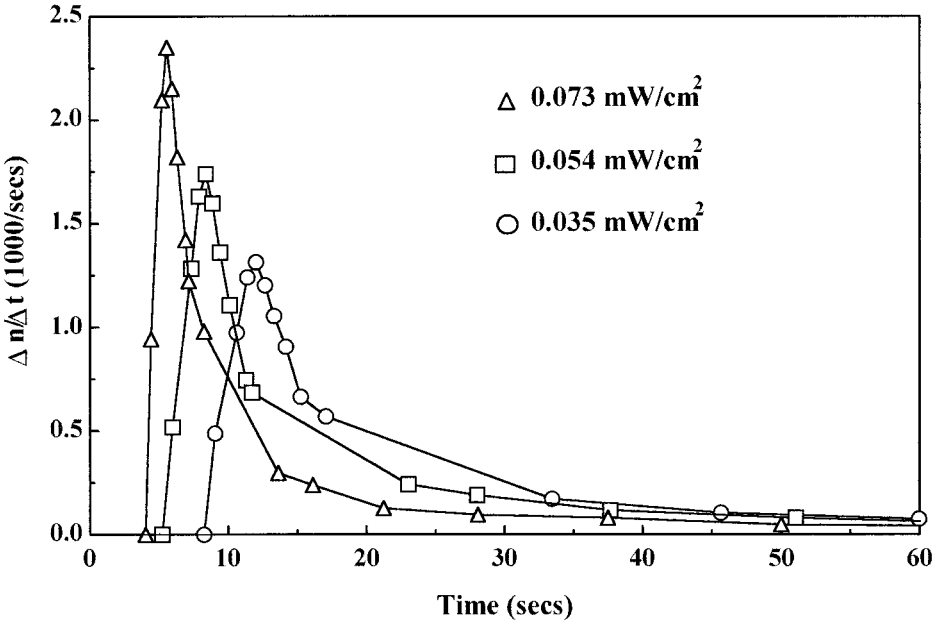

Figure 3 $\Delta n/\Delta t$ curing profiles for DPEPA samples containing 4.0% by volume Darocur 1173 and UV irradiation power densities of 0.035, 0.054, and 0.073 mW/cm^2.

The overall degree of film shrinkage over the UV illumination period can be inferred from the reference interferogram. The percent shrinkage can be calculated from the expression

$$\% \text{ shrinkage} = \frac{N\lambda}{n_r l} \times 100 \qquad (7)$$

where N is the number of oscillations over the course of the reference interferogram, λ is the wavelength of the light source, n_r is the refractive index of the uncured sample (measured with an Abbe refractometer), and l is twice the thickness of the photocured film (measured with a micrometer). For all the samples photocured in this study, the percent shrinkage fell in the range of 0.9–1.5%. No correlation was observed between the degree of shrinkage and the UV illumination intensities and/or the photoinitiator concentrations used here.

Curing Profiles

Figure 3 shows how $\Delta n/\Delta t$ varies as a function of cure time for a sample containing 4.0% Darocur; three data sets are given at UV irradiation power densities of 0.035, 0.054, and 0.073 mW/cm^2. Figure 4 shows similar plots for samples containing 2.0, 4.0, and 8.0% Darocur and a constant UV irradiation power density of 0.054 mW/cm^2. An $\sim$ 8% uncertainty exists for the $\Delta n/\Delta t$ values in these plots; this error is primarily due to the uncertainty in determining $t_2 - t_1$ from the sample and reference interferograms. All plots reveal the time lag after UV illumination where $\Delta n/\Delta t$ remains equal to zero. The duration of this time lag decreases as the UV irradiation intensity increases and as the concentration of photoinitiator increases. The time lag is followed by a rapid increase in $\Delta n/\Delta t$. The maximum value of $\Delta n/\Delta t$ increases with UV power and photoinitiator concentration.

Two time scales are apparent in the $\Delta n/\Delta t$ decays plotted in Figures 3 and 4. A dual time-scale curing profile is expected for any polymer reaction that passes through a gel point. (The refractive index variation will "freeze-out" along with the polymer reaction.) Gel time values can be roughly estimated from the $\Delta n/\Delta t$ curing profiles in Figure 3 and yield 8, 12, and 16 s for UV illumination power densities of 0.073, 0.054, and 0.035 mW/cm^2, respectively.

Inhibition of Photocuring

The time lag that appears at the beginning of each sample interferogram (or equivalently each $\Delta n/\Delta t$ curing profile) is a direct result of inhibition of the polymerization reaction by dissolved molecular oxygen and the MEHQ resin inhibitor. (Both of these species are present in the samples at $\sim 10^{-3}$ M concentrations.)[19–22] The molecular

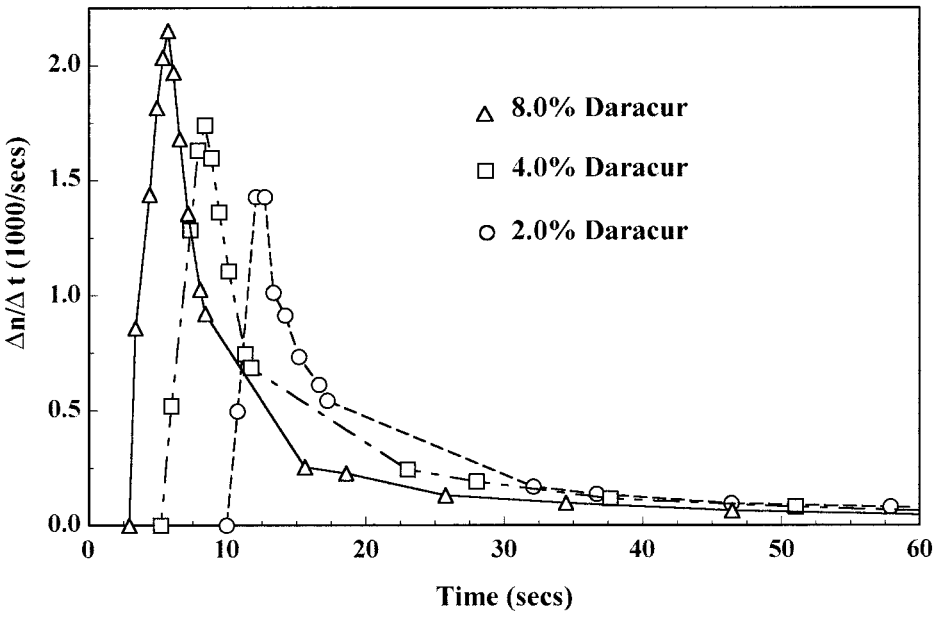

Figure 4 $\Delta n/\Delta t$ curing profiles for DPEPA samples containing 2.0, 4.0, and 8.0% by volume Darocur 1173 and a constant UV irradiation power density of 0.054 mW/cm^2.

oxygen and MEHQ in a photocurable sample will both inhibit photopolymerization by scavenging initiator radicals at a rate that is considerably greater than the rate of reaction between initiator radicals and monomer.[22] Subsequently, the photocuring reaction will not begin until nearly all the inhibitors have been consumed. The inhibition period can be minimized by using large UV illumination intensities, large photoinitiator concentrations, and/or the addition of highly oxidizable species to the photocurable formulation. The mechanisms of oxygen inhibition have been the subject of several previous investigations.[19–22] Studies by Decker and Jenkins[21] reveal that the use of high UV illumination intensities gives rise to a multistep peroxidation radical consumption mechanism.

The kinetics of inhibition can be characterized in the systems studied here by measuring the magnitude of the inhibition period as a function of UV irradiation intensity and photoinitiator concentration. The inhibition period (t_i) was directly obtained from our data as the time that transpires before the beginning of oscillations in the sample interferogram. The high concentration of photoinitiator, the weak absorption of the samples at 360 nm, and the relatively low UV illumination intensities being used in these experiments suggest that a steady-state concentration of initiator radicals should exist throughout the inhibition period. (Under these conditions, the amount of photoinitiator consumed by UV excitation is negligible over the inhibition period.) The consumption of inhibitors by a steady-state concentration of initiator radicals will occur according to a pseudo-first-order rate law in which the rate is directly proportional to the UV illumination intensity (I_o) and the photoinitiator concentration. As such, plots of t_i versus $1/I_o$, as well as plots of t_i versus reciprocal photoinitiator concentration, should be linear if pseudo-first-order kinetics are being followed. Experimental values of t_i are plotted against ($1/I_o$) in Figure 5 and against reciprocal photoinitiator concentration in Figure 6, and the linearity of these plots support a first-order inhibitor consumption mechanism in these systems. (The chain peroxidation mechanism studied by Decker and Jenkins[21] is not active under the low UV illumination conditions used here.)

CONCLUSIONS

A novel interferometric method of investigating polymer curing kinetics was demonstrated and applied to the study of UV photocuring. The recorded interferograms and corresponding $\Delta n/\Delta t$ curing profiles were found to be appropriately reproducible from trial to trial. Systematic comparisons of the $\Delta n/\Delta t$ curing profiles were made as a function of UV illumination intensity and

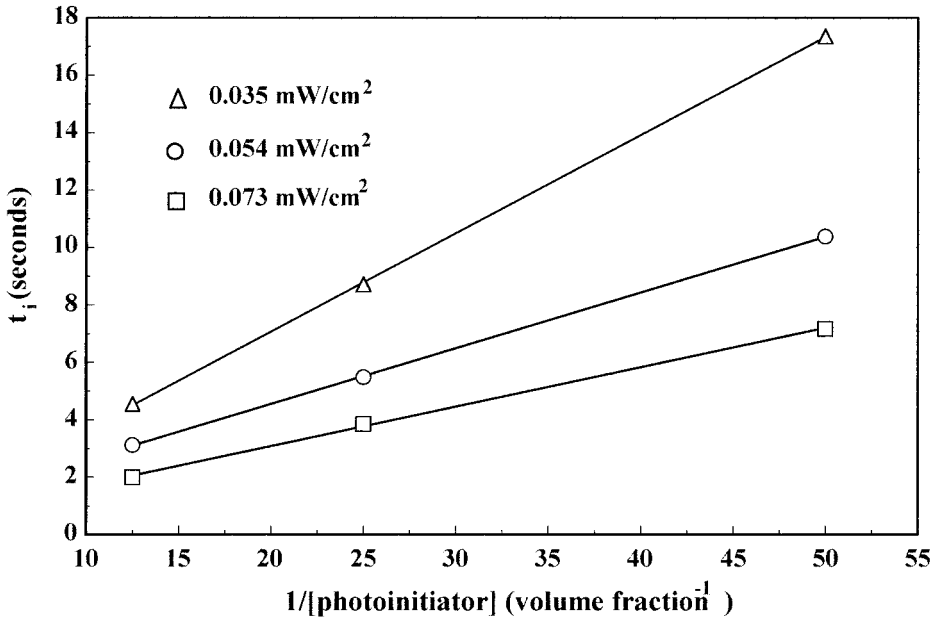

Figure 5 Plots of inhibition time (t_i) versus 1/[photoinitiator] at UV irradiation power densities of 0.035, 0.054, and 0.073 mW/cm^2. The solid lines are linear least squares fits to the data points.

photoinitiator concentration. Several advantages of interferometry were demonstrated that establish the method as a viable means of studying cure kinetics. Quality data can be obtained at high acquisition rates, permitting the study of fast polymerization reactions. Several stages of the curing process can be characterized from each sample and reference interferogram pair, including photopolymerization inhibition, the onset and degree of film shrinkage, and the determination

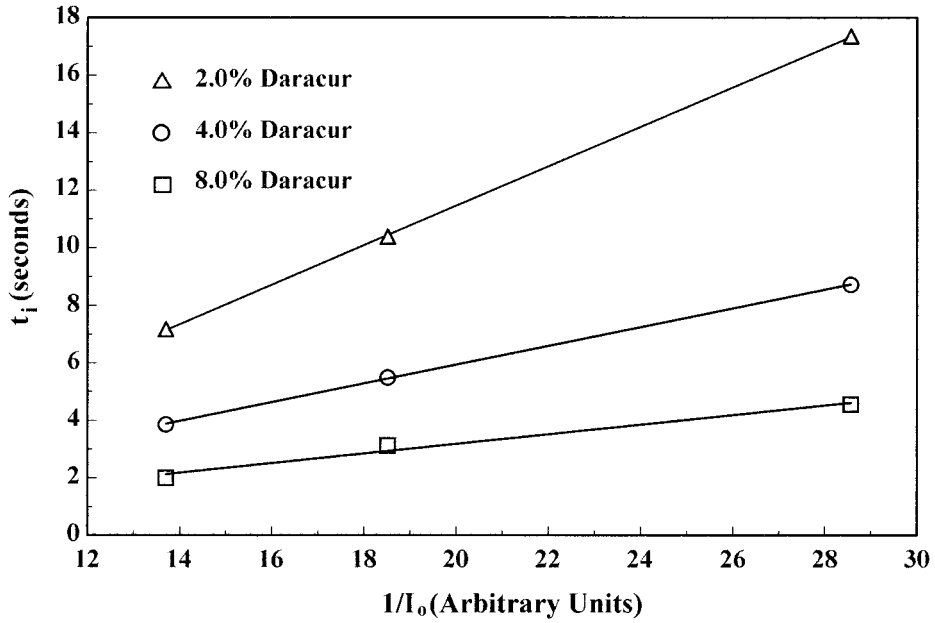

Figure 6 Plots of inhibition time (t_i) versus $1/I_o$ for DPEPA samples containing 2.0, 4.0, and 8.0% by volume Darocur 1173. The solid lines are linear least squares fits to the data points.

of the gel time. Finally, the cost of the described interferometric apparatus is minimal: the components can be purchased at a total expense of ~ $1800, excluding the data acquisition hardware/software and the UV source (Edmund Scientific, Barrington, NJ; Vere Inc., New Kensington, PA).

Future studies will focus on a number of improvements to the interferometer. For example, the film thickness employed in this study (~ 200 μm) was somewhat larger than the thickness used in most industrial photocurable coatings, which can range from 20 to 125 μm. A moderately thick film thickness was used here because the sensitivity of interferometric measurements is directly proportional to thickness; halving the film thickness will halve the number of oscillations observed in the interferogram. A simple means of extending interferometric measurements to less thick films involves using a shorter wavelength light source, such as a green or blue laser.

Additional improvements in sensitivity can be attained by stabilizing the interferometer against residual room vibrations and thermal expansion of the optical mounts. Vibrations produce sudden jumps in the interferogram signal and thermal expansions produce a slow drift in the interferogram signal. Stabilization against these noise sources can be accomplished by mounting mirror M3 (Fig. 1) to a piezoelectric crystal. This crystal can be driven by an error signal that is created by comparing the "noisy" reference detector voltage to a standard voltage. (The error signal is processed with a feedback circuit and used as input to a piezoelectric crystal controller.) The oscillations that remain in the signal interferogram after this correction can then be used to directly evaluate $\Delta n/\Delta t$ throughout the curing process.

One last improvement involves the sample cell arrangement. The presence of a Teflon spacer between the windows produces a force that opposes film shrinkage. As such, one can question whether the magnitude of this counterforce is negligible in our current cell configuration. The relatively low percent of shrinkage measured for the samples in this work (~ 1%) suggests that the Teflon spacer reduced the inherent degree of shrinkage of these films. Future studies will clarify this issue by utilizing a softer, silicon rubber spacer. In this fashion, we hope to simulate the type of "free-shrinkage" that occurs on an open substrate. This improvement, along with the above mentioned piezoelectric interferometer stabilization, should allow for a more confident interpretation of the refractive index curing profiles, leading to the characterization of long timescale densification in these films.

The authors are grateful to Ronald Obie of The Woods Coating Research Group and Drs. Tom Lick and Kevin Riggs of the Physics Department of Stetson University for contributing equipment, materials, and ideas in support of this project.

REFERENCES

1. Hashimoto, K.; Saraiya, S. J Radiat Curing 1981, 8, 4.
2. Decker, C. J Coatings Technol 1987, 59, 97.
3. Decker, C.; Moussa, K. J Coatings Technol 1993, 65, 49.
4. Koleske, J. V. J Coatings Technol 1997, 69, 29.
5. Allen, G. M.; Drain, K. R. In Radiation Curing of Polymeric Materials; Hoyle, C. E.; Kinstle, J. F., Eds.; American Chemical Society: Washington, D.C., 1990; p 242.
6. Fan, L. H.; Hu, C. P.; Zhang, Z. P.; Ying, S. K. J Appl Polym Sci 1996, 59, 1417.
7. McCrackin, F. L.; Passaglia, E.; Stromberg, R. R.; Steinberg, H. L. J Res Natl Bur Stand A Phys Chem 1963, 67A, 363.
8. Beaucage, G.; Composto, R.; Stein, R. S. J Polym Sci Part B Polym Phys 1993, 31, 319.
9. Huang, J.; Huang, X.; Liu, H. J Appl Polym Sci 1997, 65, 2095.
10. Shimbo, M.; Ochi, M.; Arai, K. J Coatings Technol 1984, 57, 45.
11. Wingard, C. D.; Beatty, C. L. J Appl Polym Sci 1990, 40, 1981.
12. Russell, G. A.; Skiens, W. E. In Radiation Curing of Polymeric Materials; Hoyle, C. E.; Kinstle, J. F., Eds.; American Chemical Society: Washington, D.C., 1990; p 284.
13. Wisnosky, J. D.; Fantazier, R. M. J Radiat Curing 1981, 8, 16.
14. Shimbo, M.; Ochi, M.; Shigeta, Y. J Appl Polym Sci 1981, 26, 2265.
15. Beysens, D.; Calmettes, P. J Chem Phys 1977, 66, 766.
16. Dannenberg, H. SPE J 1959, 875 (1959).
17. Krause, S.; Lu, Z.-H. J Polym Sci Polym Phys 1981, 19, 1925.
18. Jordan, O. P.; Marquis–Weible, F. Appl Opt 1996, 35, 6146.
19. Decker, C.; Fizet, M.; Faure, J. Org Coating Plast Chem 1980, 42, 710.
20. Decker, C. J Appl Polym Sci 1983, 28, 97.
21. Decker, C.; Jenkins, A. D. Macromolecules 1985, 18, 1241.
22. Vesley, G. F. J Radiat Curing 1986, 13, 4.